Paper #4B03

# Mechanisms of Concurrent-Flow Flame Spread Over Solid Fuel Beds

Linton K. Honda and Paul D. Ronney
Department of Aerospace and Mechanical Engineering
University of Southern California, Los Angeles, CA 90089-1453

Address correspondence to:

Prof. Paul Ronney
Department of Aerospace and Mechanical Engineering
University of Southern California
Los Angeles, CA 90089-1453
(213) 740-0490
(213) 740-8071 (fax)
ronney@usc.edu

Word count

| | | |
|---|---|---|
| Text: | = | 2550 words (counted by Microsoft Word 98) |
| Equations: 15 | = | 504 words (1a, 1b, 2a, 2b, 5, 6a, 7a, 7b, 8 counted double) |
| References: | = | 207 words (counted by Microsoft Word 98) |
| Figures: 6 | = | 1500 words (Figures 3, 5, 6 counted as 300 words each) |
| Tables: 3 x 200 | = | 600 words |
| **Total:** | **=** | **5361 words** |

Presentation preference: Oral presentation

Colloquium topic area: Fire research, flames spread, fire suppression

To be presented at
*The Twenty-Eighth International Symposium on Combustion,*
Edinburgh, Scotland, July 31 - August 4, 2000.
(To appear in *Proceedings of the Combustion Institute*, Volume 28, 2000)

# Mechanisms of Concurrent-Flow Flame Spread Over Solid Fuel Beds

Linton Honda and Paul D. Ronney
Department of Aerospace and Mechanical Engineering
University of Southern California, Los Angeles, CA 90089-1453

## ABSTRACT

It is proposed that concurrent-flow flame spread over solid fuel beds will be steady under conditions where heat and momentum losses to the sides of the fuel samples and/or surface radiative losses are significant. These losses are argued to be unavoidable because the flame length will grow until these losses balance the heat and momentum generation rates. Approximate relations (with no adjustable parameters or necessity for supplemental measured quantities such as heat fluxes or pyrolysis times) are derived for steady spread rates in the presence of these losses for laminar and turbulent flow, buoyant and forced convection, and thin and thick fuels. Experimental tests of these relations were conducted for upward flame spread over thermally-thin fuels. Varying pressures, oxygen mole fractions and diluents were employed to cover a seven-decade range of Grashof number. These experiments generally support the validity of the proposed mechanisms.

## Introduction

Flame spread over solid fuels is characterized as opposed-flow, where flames propagate opposite convection (corresponding to downward flame spread when buoyant convection dominates forced convection), or concurrent-flow (corresponding to upward spread.) Opposed-flow spread is reasonably well understood [1, 2, 3, 4] since the spread rate ($S_f$) is typically steady due to balances between upstream diffusion and downstream convection of thermal energy. In contrast, for concurrent-flow spread, convective and diffusive transport are in the same direction, thus the fuel surface area exposed to high-temperature combustion products increases with time, leading to accelerating spread [2, 3]. Consequently, concurrent-flow flame spread theory is less developed, but has great practical importance to upward flame spread in building fires.

Using boundary-layer analyses, Fernandez-Pello [3] predicts that flame length (L) and $S_f$ for concurrent flow ($S_{f,con}$) increase indefinitely with time (t) (Table 1.) Delichatsios and collaborators [5] also examined unsteady concurrent-flow spread. In contrast, some experiments using thermally-thin [6, 7] and thermally-thick [3, 8, 9] fuels show steady L and $S_{f,con}$. The analyses assumed adiabatic spread across infinitely wide samples, thus heat losses and lateral momentum losses were neglected. With such losses, the boundary layer thickness ($\delta$) could not grow substantially larger than the sample width (W) - one could not expect 10 cm thick boundary layers on 1 cm wide fuel samples. If $\delta$ is limited, then L and $S_f$ are also limited. Even for infinitely wide samples, L could not grow indefinitely because surface radiative losses would eventually exceed heat generation rates. Both assertions arise because for boundary layer flows the fuel bed heat flux (Q), thus fuel vapor generation rates and total heat generation rates, increase more weakly than linearly with L, whereas heat and lateral momentum losses increase roughly linearly with L. (Markstein and deRis [10] suggested that for thermally-thin beds, fuel burnout could limit $S_f$, but not for practical sample dimensions.) Hence, we propose

I. For sufficiently narrow fuel beds, L grows until $\delta \approx W$, when transverse heat and momentum losses prevent further growth of L, which limits Q and thus $S_f$.

II. For sufficiently wide fuel beds, L grows until surface radiative loss[1] is comparable to Q, when these losses prevent further growth of L, which limits Q and thus $S_f$.

We designate these *convectively-stabilized* and *radiatively-stabilized* flames. Although heat and momentum losses are considered, no finite-rate chemistry effects are considered, consequently, these hypotheses apply only far from extinction conditions.

In this work simple models of loss-limited concurrent-flow flame spread are developed based on these hypotheses. Experiments are conducted to test the resulting predictions. We emphasize there are no adjustable parameters nor necessity for supplemental empirical quantities such as surface heat fluxes [9, 10] or pyrolysis times [5].

## Modeling predictions

### Flame lengths

Boundary-layer analyses are appropriate for concurrent-flow flame-spread analyses [2, 3], thus for forced-convection flame spread, we assume $\delta = LAR e_L^{-a}$ and $Nu_L = BRe_L^{b}$ (A, B, a, b constant), where $Nu_L$ is the length-averaged Nusselt number, $Re_L \equiv UL/\nu_g$ the Reynolds number, U the forced convection velocity and $\nu_g$ the kinematic viscosity. For buoyant-convection dominated spread, we assume $\delta = LCGr_L^{-c}$ and $Nu_L = DGr_L^{d}$, where $Gr_L \equiv gL^3/\nu_g^2$ is the Grashof number. We assume Prandtl numbers (Pr) close to unity and that the thermal expansion term generally present in $Gr_L$ is close to unity, which is reasonable since the product density is 5-8 times smaller than the reactant density. For laminar flow, classical models yield (based on the momentum boundary layer thickness, for Pr=0.72) A=0.664, a=1/2, B=0.595, b=1/2 [11] and (defining $\delta$ as the horizontal distance from the velocity maximum) C=1.37, c=1/4, D=0.476, d=1/4 [12]. For turbulent flow A=0.14, a=1/7, B=0.0131 and b=6/7 [13] and (at $Gr_L < 10^{10}$,

[1]We treat radiative loss simply as a surface loss with no gas-phase reabsorption. Our estimates indicate this approximation is reasonable since solid fuels emit as roughly gray bodies whereas gases absorb only in narrow spectral bands. Optically-thin gas-phase radiation was considered as another loss mechanism but rejected because it is isotropic, hence the loss is balanced by increased radiative flux to the fuel bed, yielding little net effect on $S_f$. Gas-phase radiation affects the mass burning rate of fully developed fires on thick vertical walls, but we are analyzing only $S_f$ for developing fires.

corresponding to all conditions we could study), C=0.030, c=0.10 [14, 15], D=0.474 and d=0.25 [16].

Hypothesis I states $\delta \approx W$, consequently

$$L/W \approx A^{-1/(1-a)}\,\mathrm{Re}_W^{a/(1-a)};\ Nu_L \approx BA^{-b/(1-a)}\,\mathrm{Re}_W^{b/(1-a)};\mathrm{Re}_W \equiv \frac{UW}{\nu_g} \quad \text{(forced convection)} \quad (1a)$$

$$L/W \approx C^{-1/(1-3c)}Gr_W^{c/(1-3c)};\ Nu_L \approx DC^{-3d/(1-3c)}Gr_W^{d/(1-3c)};\ Gr_W \equiv \frac{gW^3}{\nu_g^{\,2}} \quad \text{(buoyant convection)} \quad (1b).$$

where all gas properties are temperature-averaged as discussed later. Note that L/W and $Nu_L$ are expressed through known experimental conditions $Re_W$ or $Gr_W$ rather than unknown $Re_L$ or $Gr_L$.

Hypothesis II states that $Q=(Nu_L\lambda_g/L)(T_f-T_v)$ equals the radiative loss from the bed $(H)=\sigma\varepsilon(T_v^4-T_\infty^4)$, where $\lambda_g$, $\sigma$, $\varepsilon$, $T_f$, $T_v$, $T_\infty$, are the gas thermal conductivity, Stefan-Boltzman constant, bed emissivity, flame temperature [1], vaporization temperature and ambient temperature, respectively. Thus

$$L/W \approx B^{1/(1-b)}Pl_W^{1/(1-b)}\,\mathrm{Re}_W^{b/(1-b)};\ Nu_L \approx B^{1/(1-b)}Pl_W^{b/(1-b)}\,\mathrm{Re}_W^{b/(1-b)} \quad \text{(forced convection)} \quad (2a)$$

$$L/W \approx D^{1/(1-3d)}Pl_W^{1/(1-3d)}Gr_W^{d/(1-3d)};Nu_L \approx D^{1/(1-3d)}Pl_W^{3d/(1-3d)}Gr_W^{d/(1-3d)} \quad \text{(buoyant convection)} \quad (2b),$$

where $Pl_W \equiv \lambda_g(T_f-T_v)/W\varepsilon\sigma(T_v^4-T_\infty^4)$ is the *Planck number*. Equations 1-2 then yield predictions for L/W and $Nu_L$ (Table 2).

**Spread rates**

$S_{f,con}$ is estimated by equating Q to the rate of fuel bed enthalpy increase $(=\rho_s C_{p,s}\tau_s(T_v-T_\infty)WS_f$, where $\rho_s$, $C_{p,s}$ and $\tau_s$ are the fuel bed density, heat capacity and thickness, respectively). Thus, for thermally-thin fuels,

$$S_{f,con}/S_{f,opp} = \frac{4}{\pi}Nu_L;\ S_{f,opp} = \frac{\pi}{4}\frac{\lambda_g}{\rho_s C_{p,s}\tau_s}\left(\frac{T_f-T_v}{T_v-T_\infty}\right) \quad (3)$$

where for compactness $S_{f,con}$ is referenced to $S_f$ for laminar, opposed-flow spread ($S_{f,opp}$) [17].

For thick fuels $S_{f,con}$ is estimated by substituting the solid thermal penetration depth ($\tau_p$) [1] for $\tau_s$ in Eq. 3. $\tau_p$ is estimated by equating Q to the heat flux from the fuel surface into the

bed $=\lambda_s(T_v-T_\infty)/\tau_p$, where $\lambda_s$ is the solid thermal conductivity. This yields

$$\tau_p = \frac{L}{Nu_L}\frac{\lambda_s}{\lambda_g}\frac{T_v - T_\infty}{T_f - T_v} \tag{4}.$$

With $\tau_p=\tau_s$, Eqs. 3-4 yield

$$S_{f,con}\Big/S_{f,opp} = Nu_L^2\left(\frac{L}{W}\right)^{-1}\left(\frac{U_{opp}W}{\nu_g}\right)^{-1};\ S_{f,opp} = U_{opp}\frac{\rho_g C_{p,g}\lambda_g}{\rho_s C_{p,s}\lambda_s}\left(\frac{T_f - T_v}{T_v - T_\infty}\right)^2 \tag{5}.$$

Combining Eqs. 3-5 with $Nu_L$ from Table 2 yields predictions for $S_{f,con}$ (Table 3). For forced flow, $U_{opp}$ = U is prescribed; for buoyant flow, $U_{opp}$ cannot be prescribed; we employ the estimate $U_{opp}\approx E^{1/3}(g\nu_g)^{1/3}$, where $E\approx(0.72/Pr)(T_f-T_v)/T_\infty$ [1]. This estimate of $U_{opp}$ for buoyant flow is incorporated into thick-fuel predictions (Table 3).

This analysis is readily extended to *unsteady* spread by neglecting loss mechanisms and setting $S_f=dL/dt$ rather than $S_f=$constant. This leads to first-order differential equations for L(t). For example, for thin fuels under buoyant flow,

$$S_{f,con}(t) \approx \frac{dL}{dt} \approx \frac{4}{\pi}Nu_L(t)S_{f,opp} \approx \frac{4C}{\pi}Gr_L(t)^c S_{f,opp} = \frac{4C}{\pi}Gr_W^c\left(\frac{L(t)}{W}\right)^{3c} S_{f,opp} \tag{6a}$$

which has the solution

$$S_{f,con} = \frac{1}{1-3c}\left(\frac{4C(1-3c)}{\pi}\left(\frac{Gr_W}{W^3}\right)^c S_{f,opp}\right)^{1/1-3c} t^{3c/1-3c} \tag{6b}$$

For laminar flow (c=1/4),

$$S_{f,con} = 4\left(\frac{C}{\pi}\right)^4 S_{f,opp}^4\frac{Gr_W}{W^3}t^3 \tag{6c}$$

which has the form $S_f \sim t^3$ proposed by Fernandez-Pello (Table 1). The other relations in Table 1 can be derived similarly. Thus, our proposed approach is considered quite general.

**Transitions between regimes**

Transition between laminar and turbulent flame spread occurs when $Re_L$ or $Gr_L$ exceeds critical values, denoted $Re_L^* \approx 5 \times 10^5$ and $Gr_L^* \approx 4 \times 10^8$. By writing $Re_W = Re_L/(L/W)$ and $Gr_W = Gr_L/(L/W)^3$, with expressions for L/W taken from Table 2, we infer at transition, for convectively-stabilized flames

$$\mathrm{Re}_W = A\left(\mathrm{Re}_L^*\right)^{1-a} \text{ (forced); } Gr_W = C^3\left(Gr_L^*\right)^{1-3c} \text{ (buoyant)} \qquad (7a),$$

and for radiatively-stabilized flames

$$\mathrm{Re}_W = B^{-1}\left(\mathrm{Re}_L^*\right)^{1-b} Pl_W^{-1} \text{ (forced); } Gr_W = D^{-3}\left(Gr_L^*\right)^{1-3d} Pl_W^{-3} \text{ (buoyant)} \qquad (7b).$$

Transition between convective and radiative stabilization occurs when the predicted L are equal, thus

$$Pl_W = \frac{1}{B}\left(\frac{1}{A}\right)^{1-b/1-a} \mathrm{Re}_W^{\,a-b/1-a} \text{ (forced); } Pl_W = \frac{1}{D}\left(\frac{1}{C}\right)^{1-3d/1-3c} Gr_W^{\,c-d/1-3c} \text{ (buoyant)} \qquad (8).$$

Figure 1 shows flame spread regimes for buoyant flow, obtained by mapping these transitions into ($Gr_W$, $Pl_W$) space and eliminating inconsistent transitions (for example direct transition from convective stabilization / laminar flow (CL) to radiative stabilization / turbulent flow (RT)). Figure 1 also shows combinations of $Gr_W$ and $Pl_W$ accessible by varying W for ambient air, 0.25 atm $O_2$-He, and 3 atm $O_2$-$SF_6$ atmospheres, the latter two having the highest and lowest $\nu_g$ we employed. (In Fig. 1 and subsequent predictions, $\lambda_g$ and $\nu_g$ are taken as averages of values at $T_\infty$ and $T_f$ assuming $\lambda_g \sim T^{0.75}$ and $\nu_g \sim T^{1.75}$.) For small W, CL spread always applies. For high-$\nu_g$ atmospheres, only transition to radiative stabilization / laminar flow (RL) occurs. For lower $\nu_g$, transition to RT occurs, possibly with intermediate RL or CT regimes for marginal ranges of W.

**Comparison with previous results**

Relatively few experimental or computational results are available for comparison with these predictions. Thin-fuel buoyant-flow experiments at low pressure (P) ([6], Fig. 14) in $30\%O_2/70\%N_2$ atmospheres with small W (10 mm) show $S_{f,con}\sim P^{1.8}$. This is close to our prediction $S_f\sim P^2$ for CL or RL spread (with c=d=1/4, $S_f\sim Gr_W^{1}$ (CL) or $S_f\sim Gr_W^{1}Pl_W^{3}$ (RL); since $Gr_W\sim\nu_g^{-2}\sim P^2$ and $Pl_W\sim\lambda_g^{1}\sim P^0$, $S_f\sim P^2$). In contrast, for downward (opposed-flow) flame spread, $S_f\sim P^0$ [1, 18]. Concurrent laminar forced-flow experiments [8, 9] over wide, thermally-thick PMMA sheets show $S_f\sim U^1$ behavior, consistent with Table 3 for thick CL or RL spread since for a=b=1/2, $S_{f,con}\sim Re_W^{0}S_{f,opp}\sim U^1$. (In [9], grid turbulence was employed, but $Re_L<Re_L^{*}$ for all test conditions, plus turbulence intensity had little effect on $S_f$, thus laminar values of a and b apply). Adiabatic analyses (Table 1) also predict $S_{f,con}\sim U^1$, but predict $L\sim t^1$, whereas our non-adiabatic analysis predicts steady $L\sim Re_W^{1}$. Unfortunately, no time-dependent data on L were reported in [8, 9] to compare adiabatic and non-adiabatic models. Ferkul and Tien [19] modeled concurrent forced-flow flame spread over two-dimensional (infinitely wide, thus convective stabilization cannot apply) thermally-thin samples with surface radiative loss and predicted steady spread with $S_{f,con}\sim U^1$ (whereas $S_{f,opp}\sim U^0$ [1]) and $L\sim U^1$, consistent with Tables 2-3 for RL spread. In contrast, **adiabatic** analyses predict $S_{f,con}\sim t^1$ for these assumptions (Table 1). Jiang *et al.* [20] found $S_{f,con}\sim g^1$ and $L\sim g^1$ for concurrent buoyant spread, again consistent with RL predictions.

## Experiments

**Apparatus and procedures**

Since few data are available for comparison with Tables 2-3, but these data are generally consistent with predictions, comprehensive data sets were generated for thin fuels under buoyant convection by measuring the effects of W, P, $\tau_s$ and diluent type on $S_{f,con}$. To obtain small $Gr_w$, small W and P were employed. These conditions cause flame quenching, hence elevated oxygen concentrations (at least 4 mole percent above quenching limits) were used, enabling steady upward spread for $Gr_w$ down to $3x10^2$ in $O_2$-He atmospheres at low pressure (large $\nu_g$). To obtain large $Gr_W$, $CO_2$ and $SF_6$ diluents at high pressure (small $\nu_g$) with large W were employed. While large $Gr_W$ results in large flame length, using a 2 m tall chamber enabled steady spread (defined as steady $S_f$ and L) at $Gr_w$ up to $3x10^9$, corresponding to W=41 cm in ambient air. (At still larger $Gr_w$, steady spread was not reached within the available distance; such data were

discarded.) Consequently, a 7-decade range of $Gr_W$ exhibiting steady spread could be examined. Steady spread was defined to be when the pyrolysis front and flame leading edge propagated at identical and steady rates with constant flame length (L). The necessary reference values of $S_{f,opp}$ were measured for downward propagation over samples sufficiently wide that $S_{f,opp}$ was independent of W.

The apparatus employed was similar to that used in prior studies [18] except for the taller chamber (2 m). The chamber gases were generated via the partial pressure method. Kimwipes fuel samples ($\rho_s\tau_s = 0.0018$ g/cm$^2$) of single or double thickness were held by aluminum clamps to inhibit edge burning and ignited by electrically heated wires. 50 μm diameter type S thermocouples having 50 millisecond typical response time were attached to the clamp. Thermocouple voltages were recorded by a PC-based data acquisition system. The flames were recorded on video. $S_f$ was inferred from video records or thermocouple data; these were identical within experimental uncertainty. Estimated uncertainties in $S_f$, temperature, $O_2$ mole fraction and total pressure are 5%, 5%, 1%, and 0.5%, respectively.

**Results**

Figure 2 shows the effect of W on $S_{f,con}$ for ambient air. At low $Gr_W$, $S_{f,con} \sim W^{2.83}$, thus $S_{f,con}/S_{f,opp} \sim Gr_W^{0.94}$, close to the CL prediction (Table 3) $S_{f,con}/S_{f,opp} \sim Gr_W^{1}$. At $Gr_W > 30{,}000$, $S_{f,con} \sim W^{0.51}$, thus $S_{f,con}/S_{f,opp} \sim Gr_W^{0.17}$, close to RL or RT predictions since $S_{f,con}/S_{f,opp} \sim Gr_w^{1} Pl_w^{3} \sim W^3 W^{-3} \sim W^0$. The observed transition $Gr_W$ is close to the CL-RL prediction $Gr_W \approx 30{,}000$ (Fig. 1). This should be followed by RL-RT transition at $Gr_W \approx 90{,}000$, but this cannot be discerned because the $Gr_W$ range corresponding to RL behavior is narrow. Furthermore, there is little difference between RL and RT predictions for $S_f$ since D and d are only slightly different for laminar vs. turbulent flow.

Figure 3 shows the correlation between $S_{f,con}/S_{f,opp}$ and $Gr_W$ for all data. At low $Gr_w$, the proposed relation $S_{f,con}/S_{f,opp} \sim Gr_w^{1}$ fits each data set for a given atmosphere well, although between different atmospheres a factor of 2.5 variation in $S_{f,con}/S_{f,opp}$ is found at constant $Gr_w$. Nevertheless, the comparison is considered quite reasonable considering the wide range of experimental conditions tested. We believe much of the scatter results from varying degrees of dissociation for various atmospheres, which in turn affects temperature averaging. At higher $Gr_w$, all data bend towards horizontal, indicating $S_{f,con}/S_{f,opp} \sim Gr_w^{0}$, consistent with radiative stabilization. The transition $Gr_W$ varies from about 5,000 for the highest $\nu_g$ atmosphere tested

(30% $O_2$-He, 0.25 atm) to 200,000 for the lowest $\nu_g$ tested (46% $O_2$-$SF_6$, 3 atm). These transitions are in very good agreement with predictions (Fig. 1). $S_{f,con}/S_{f,opp}$ predictions are in very good agreement with experiments for high and intermediate $\nu_g$, though high for the lowest $\nu_g$ (3 atm $O_2$-$SF_6$ predictions are slightly off the graph).

Figure 3 shows the utility of the proposed scalings; wide ranges of $S_f$ and $Gr_W$ for varying $Pl_W$ are correlated on one plot. Effects of Lewis number [18] and other mixture properties are covered by referencing $S_{f,con}$ to $S_{f,opp}$. For convectively-stabilized flames, $T_f$ effects appear only through temperature averaging of transport properties. $T_v$ effects appear only for radiative-stabilized flames (through $Pl_W$).

Flame lengths were measured from thermocouple data (Fig. 4.) Temperatures rise sharply then plateau upon flame leading edge arrival, then fall sharply upon trailing edge passage. Note that temperature histories at two vertical locations (y=0, y=68) are very similar, indicating steady spread. L was defined as $S_f(\Delta t)$, where $\Delta t$ is the time lapse between leading and trailing edge passage at 900˚C, because this gave good agreement with visible flame lengths. (Thermocouple-based lengths were more consistent and thus preferred for quantitative measurement). The thermocouple closest to the surface (2 mm) was used because for small $\nu_g$, $\delta$ was very small, consequently, more remote thermocouples exhibited no significant temperature rise. Figure 5 shows correlations of L/W with $Gr_W$. At low $Gr_W$, most data for a given atmosphere follow the predicted $L/W \sim Gr_w^{1}$ for CL spread (Table 2), albeit with substantial scatter between different atmospheres. For large W, $L/W \sim Gr_W^{-1/3}$ as required for width-independent L.

A critical aspect of our hypotheses is that $S_f$ is determined by $Nu_L$, which in turn is determined by L. From Tables 2-3, the predicted relationships between $S_{f,con}$ and L for buoyant flow are:

$$L/W \approx \frac{1}{C}\left(\frac{4}{\pi}D\right)^{-c/d}\left(\frac{S_{f,con}}{S_{f,opp}}\right)^{c/d} \qquad \text{(convective stabilization)} \qquad (9a)$$

$$L/W \approx \left(\frac{4}{\pi}D\right)^{-1/3d} Gr_W^{-1/3}\left(\frac{S_{f,con}}{S_{f,opp}}\right)^{1/3d} \qquad \text{(radiative stabilization)} \qquad (9b)$$

Figure 6 shows the ratios of the left-hand to right-hand sides of these equations, based on measured $S_{f,con}/S_{f,opp}$ and L/W. For large $Gr_W$, agreement with RT predictions is very good; for $Gr_W$>200,000, the mean ratio is 1.63 with a standard deviation 37% of the mean. For smaller $Gr_W$, either CL or RT predictions are roughly consistent with experiments (though offset by factors of about 3), but only CL predictions are consistent with $S_f$ data (Fig. 3), as predicted by Fig. 1. Figure 1 suggests that atmospheres with the smallest $\nu_g$ might exhibit CT behavior for marginal ranges of $Gr_W$; while no data in Fig. 6 are consistent with CT predictions, intermediate $Gr_W$ ($10^4$-$10^5$) come closest, as expected based on Fig. 1. Consequently, the relationships between measured L and $S_{f,con}$ are generally consistent with our modeling hypotheses considering the transitions between regimes.

## Conclusions

Models of concurrent-flow flame spread were developed hypothesizing that for narrow fuel beds, lateral heat and/or momentum losses limit flame length, and for wide fuel beds, surface radiation losses limit flame length. These losses lead to steady rather than accelerating spread for sufficiently tall beds. Spread rate predictions were developed for thermally-thin and thermally-thick fuel beds. These results were generally in agreement with limited prior experimental and theoretical results. Upward flame spread experiments were performed for thermally-thin beds for varying width, thickness, pressure and oxygen concentration. These data generally support the proposed models. The results may be useful in developing improved models of concurrent-flow flame spread in more complex geometries, such as upward fire spread in enclosures. In future work, thermally-thick fuels will be studied, since these conditions are relevant to wall fires in buildings.

## Acknowledgments

This work was supported by NASA-Glenn under grants NAG3-1611 and NCC3-671. We thank Drs. Michael Delichatsios and Suleyman Gokoglu for helpful discussions.

## References


1. deRis, J.N., *Proc. Combust. Inst.* 12:241-252 (1968).
2. Williams, F.A., *Proc. Combust. Inst.* 16:1281-1294 (1976).
3. Fernandez-Pello, A.C., *Combust. Sci. Tech*. 39:119-134 (1984).
4. Bhattacharjee, S., West, J., Dockter, S., *Combust. Flame* 104:66-80 (1996).
5. Delicahatsios, M.A., Delichatsios, M., Chen, Y., Hasemi, Y., *Combust. Flame* 102:357-370 (1995).
6. Fernandez-Pello, A.C., Hirano, T., *Combust. Sci. Tech.* 32:1-31 (1983).
7. Grayson, G.D., Sacksteder, K.R., Ferkul, P., T'ien, J.S., *Micrograv. Sci. Tech*. 7, 187-195 (1994).
8. Loh, H.T., Fernandez-Pello, A.C., *Proc. Combust. Inst.* 20:1575-1582 (1984).
9. Zhou, L., Fernandez-Pello, A.C., *Combust. Flame.* 92:45-59 (1993).
10. Markstein, G.H., deRis, J., *Proc. Combust. Inst.* 12:1085-1097 (1972).
11. Schlichting, H., *Boundary Layer Theory*, 4th ed., McGraw-Hill, 1960.
12. Gebhart, B., Jaluria, Y, Mahajan, R.L., Sammakia, B., *Buoyancy-Induced Flows and Transport*, Hemisphere, 1988.
13. White, F.M., *Viscous Fluid Flow*, McGraw-Hill, 1974.
14. Mason, H.B., Seban, R.A., *Int. J. Heat Mass Transfer* 17:1329-1336 (1974).
15. Cheesewright, R., *J. Heat Trans.* 90:1 (1968).
16. Churchill, S.W., Usagi, R., *AIChE J.* 18:1121 (1972).
17. Delichatsios, M.A., *Combust. Sci. Tech*. 44:257-267 (1986).
18. Zhang, Y., Ronney, P.D., Roegner, E., Greenberg, J.B., *Combust. Flame* 90:71-83 (1992).
19. Ferkul, P.V., Tien, J.S. *Combust. Sci. Tech*. 99:345-370 (1994).
20. Jiang, C.-B., T'ien, J.S., Shih, H.-Y., *Proc. Combust. Inst.* 26:1353-1360 (1996).

## Tables

| Fuel Type | Buoyant convection | Forced convection |
|---|---|---|
| Thermally thin | $S_{f,con} \sim t^3$, $L \sim t^4$ | $S_{f,con} \sim t^1$, $L \sim t^2$ |
| Thermally thick | $S_{f,con} \sim t^1$, $L \sim t^2$ | $S_{f,con} \sim t^0$, $L \sim t^1$ |

Table 1. Predicted variation in spread rate ($S_{f,con}$) and flame length (L) with time (t) for laminar concurrent-flow flame spread (from [3] and references therein).

| Stabilization type | Buoyant convection | | Forced convection | |
|---|---|---|---|---|
| | $Nu_L$ | L/W | $Nu_L$ | L/W |
| Convective | $DC^{\frac{-3d}{1-3c}} Gr_W^{\frac{d}{1-3c}}$ | $C^{\frac{-1}{1-3c}} Gr_W^{\frac{c}{1-3c}}$ | $BA^{\frac{-b}{1-a}} \mathrm{Re}_W^{\frac{b}{1-a}}$ | $A^{\frac{-1}{1-a}} \mathrm{Re}_W^{\frac{a}{1-a}}$ |
| Radiative | $D^{\frac{1}{1-3d}} Pl_W^{\frac{3d}{1-3d}} Gr_W^{\frac{d}{1-3d}}$ | $D^{\frac{1}{1-3d}} Pl_W^{\frac{1}{1-3d}} Gr_W^{\frac{d}{1-3d}}$ | $B^{\frac{1}{1-a}} Pl_W^{\frac{b}{1-a}} \mathrm{Re}_W^{\frac{b}{1-a}}$ | $B^{\frac{1}{1-b}} Pl_W^{\frac{1}{1-b}} \mathrm{Re}_W^{\frac{b}{1-b}}$ |

Table 2. Predicted relations for the steady values of $Nu_L$ and L/W for forced or buoyant convection and convective or surface radiation. Predictions are the same for thermally-thin and thermally-thick fuels. Note that since $Re_w \sim W$, $Gr_w \sim W^3$ and $Pl_w \sim W^{-1}$, L is independent of W for radiatively-stabilized flames.

| Stabilization type / fuel type | Buoyant convection | Forced convection |
|---|---|---|
| Convective / thin | $\frac{4}{\pi} DC^{\frac{-3d}{1-3c}} Gr_W^{\frac{d}{1-3c}}$ | $\frac{4}{\pi} BA^{\frac{-b}{1-a}} \mathrm{Re}_W^{\frac{b}{1-a}}$ |
| Radiative / thin | $\frac{4}{\pi} D^{\frac{1}{1-3d}} Pl_W^{\frac{3d}{1-3d}} Gr_W^{\frac{d}{1-3d}}$ | $\frac{4}{\pi} B^{\frac{1}{1-b}} Pl_W^{\frac{b}{1-b}} \mathrm{Re}_W^{\frac{b}{1-b}}$ |
| Convective / thick | $\frac{D^2}{E} C^{\frac{1-6d}{1-3c}} Gr_W^{\frac{-(1-6d)}{3(1-3c)}}$ | $B^2 A^{\frac{1-2b}{1-a}} \mathrm{Re}_W^{\frac{-(1-2b)}{1-a}}$ |
| Radiative / thick | $\frac{D^{\frac{1}{1-3d}}}{E} Pl_W^{\frac{-(1-6d)}{1-3d}} Gr_W^{\frac{-(1-6d)}{3(1-3d)}}$ | $B^{\frac{1}{1-b}} Pl_W^{\frac{-(1-2b)}{1-b}} \mathrm{Re}_W^{\frac{-(1-2b)}{1-b}}$ |

Table 3. Predicted relations for steady values of $S_{f,con}/S_{f,opp}$ for thin and thick fuels, forced and buoyant convection, and convective and surface radiative loss stabilization. Since $Re_w \sim W$, $Gr_w \sim W^3$ and $Pl_w \sim W^{-1}$, $S_{f,con}$ is always independent of W for radiatively-stabilized flames.

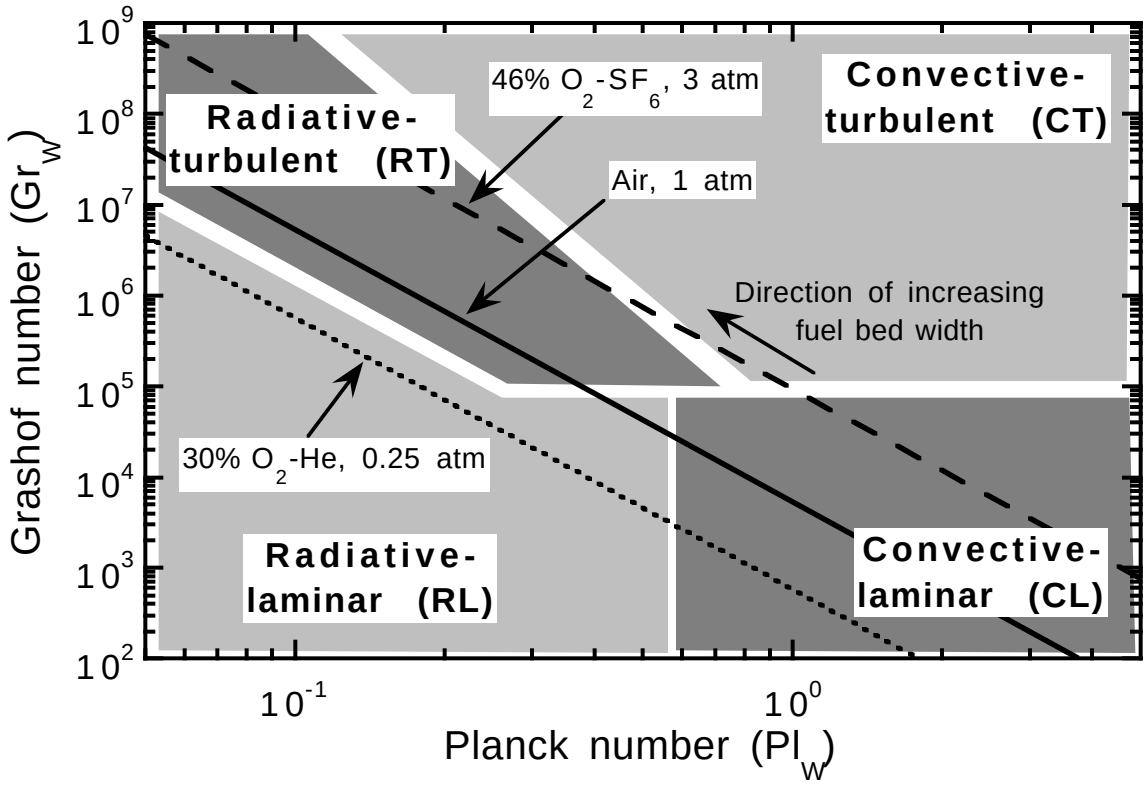


Figure 1. Predicted regimes of concurrent-flow flame spread for buoyant convection, showing the type of flow (laminar or turbulent) and type of flame stabilization (convective or radiative). Also shown are lines corresponding to fixed atmosphere but varying fuel bed width (W) for air and the atmospheres yielding the lowest and highest $Pl_W$ and $Gr_W$ tested experimentally in this work, *i.e.*, 0.25 atm $O_2$-He and 3 atm $O_2$-$SF_6$, respectively, for $T_v = 618$K, $T_\infty = 300$K and $\varepsilon = 1$.

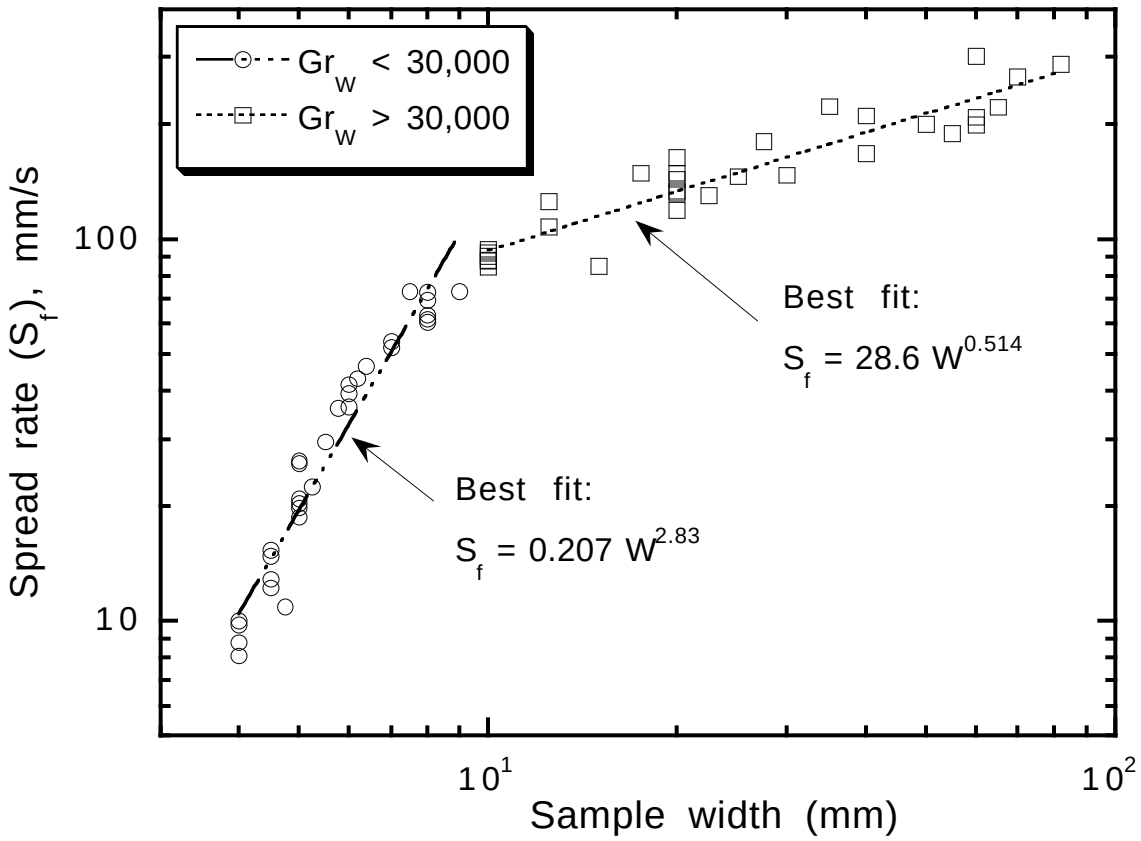


Figure 2. Effect of fuel bed width (W) on upward flame spread rate ($S_{f,con}$) for thin fuel beds burning in ambient air. Predicted results are $S_f \sim W^3$ for low $Gr_W$ and $S_f \sim W^0$ for high $Gr_W$, with a transition $Gr_W$ of 30,000.

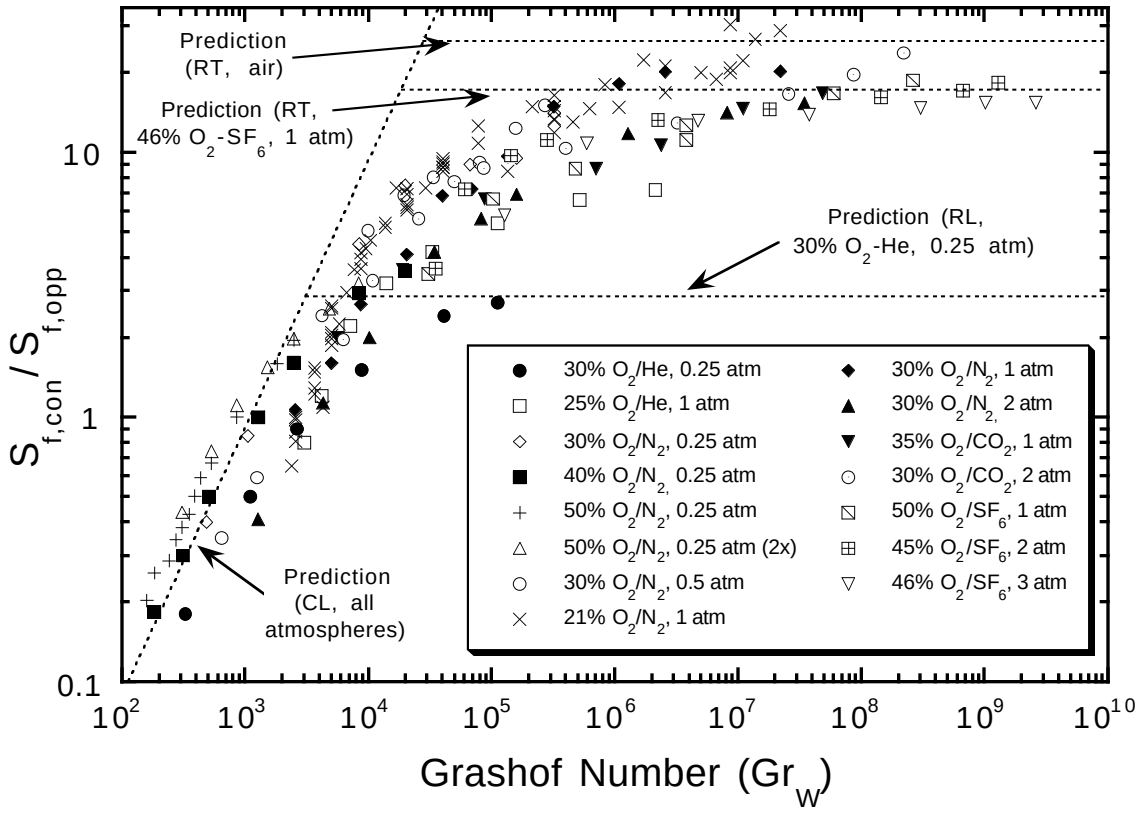


Figure 3. Correlation of steady values of $S_{f,con}/S_{f,opp}$ with $Gr_W$ for all experimental data. "2x" indicates double-thickness fuel samples.

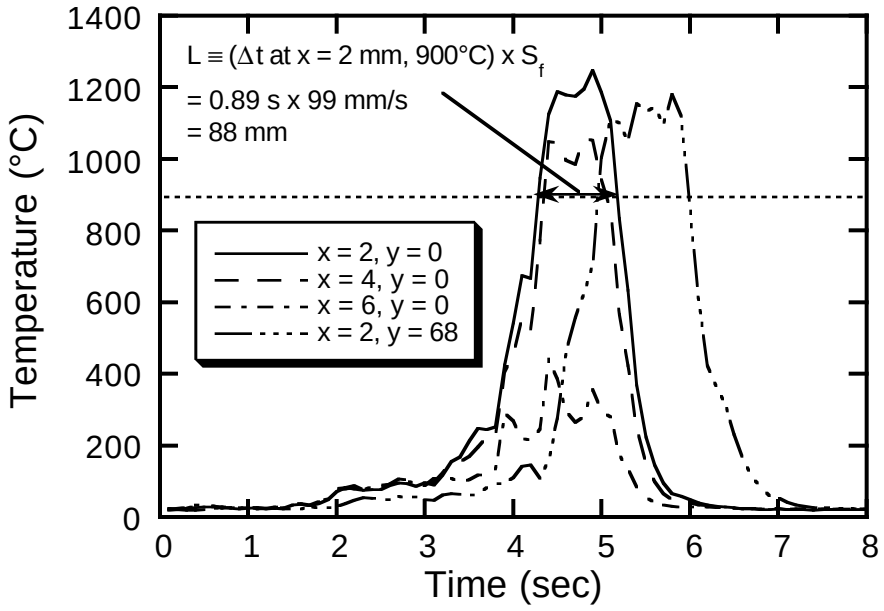


Figure 4. Example of temperature vs. time history for upward-spreading flame in air at 1 atm over a 10 mm wide fuel bed ($Gr_W$=4.5 x $10^4$). "x" values denote horizontal distance from fuel surface in mm; "y" values denote vertical distance from primary measurement station in mm.

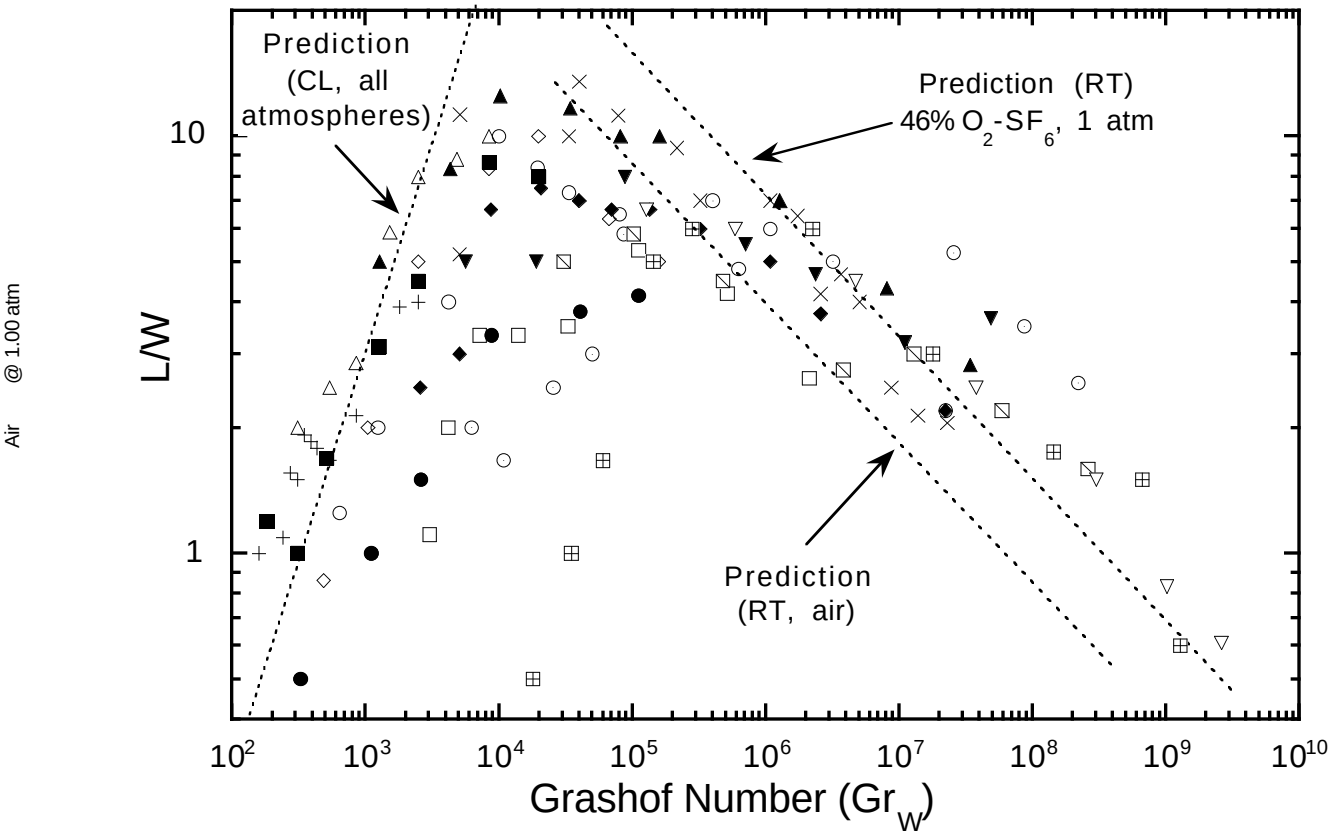


Figure 5. Correlation of steady values of L/W with $Gr_W$ for all experimental data. Legend is the same as Figure 3.

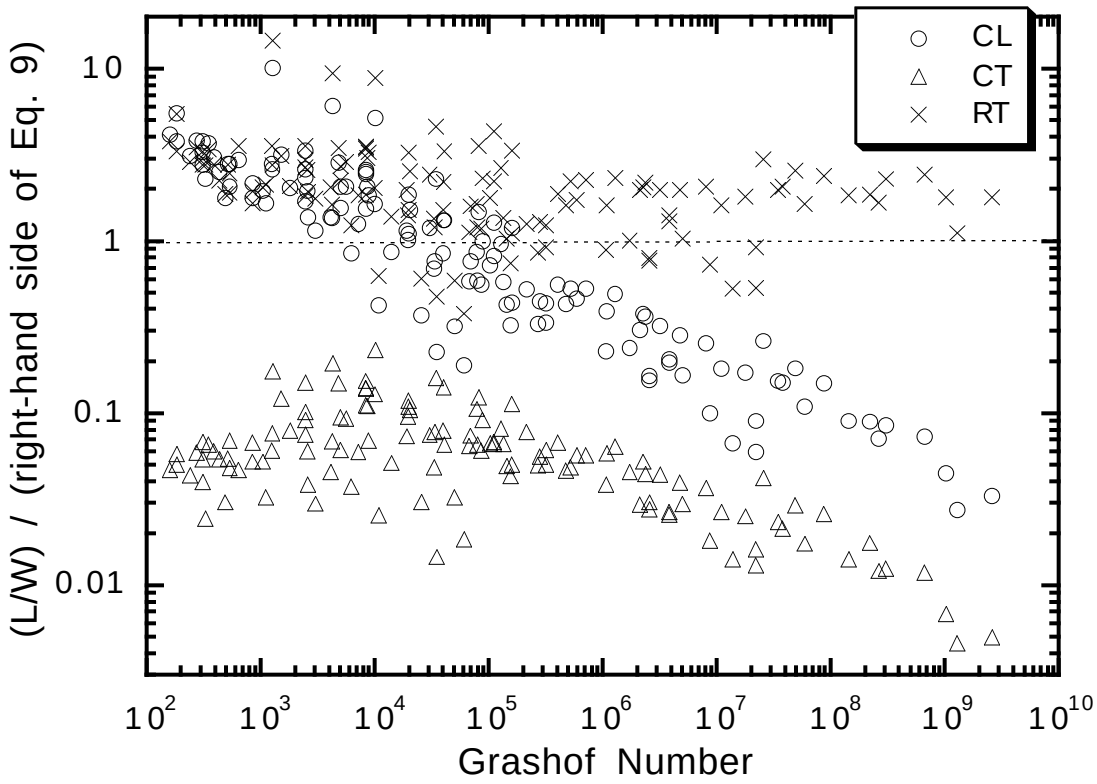


Figure 6. Ratio of measured L/W to right-hand sides of Eqs. 9a-b, showing comparison of predicted and observed correlation of L to $S_{f,con}$ for convective-laminar, convective-turbulent, and radiative-turbulent spread regimes (see Fig. 1). Dashed horizontal line indicates ideal fit of prediction to experiments.